Computers and Concrete, Vol. 2, No. 2 (2005) 111-123 111
DOI: http://dx.doi.org/10.12989/cac.2005.2.2.111

Ductility enhancement of reinforced concrete thin walls

Jang Hoon Kim†

Department of Architecture, Ajou University, Suwon 443-749, Republic of Korea
(Received October 1, 2004, Accepted March 9, 2005)

Abstract. The ductility of reinforced concrete bearing walls subjected to high axial loading and moment can be enhanced by improving the deformability of the compression zone or by reducing the neutral axis depth. The current state-of-the-art procedure evaluating the confinement effect prompts a consideration of the spaces between the transverse and longitudinal reinforcing bars, and a provision of tie bars. At the same time, consideration must also be given to the thickness of the walls. However, such considerations indicate that the confinement effect cannot be expected with the current practice of detailing wall ends in Korea. As an alternative, a comprehensive method for dimensioning boundary elements is proposed so that the entire section of a boundary element can stay within the compression zone when the full flexural strength of the wall is developed. In this comprehensive method, the once predominant code approach for determining the compression zone has been advanced by considering the rectangular stress block parameters varying with the extreme compression fiber strain. Moreover, the size of boundary elements can also be determined in relation to the architectural requirement.

Keywords: boundary element; confinement effect; dimensioning; flexure; section analysis; stress block parameter; thin RC wall.

1. Introduction

High-rise apartment buildings are typical dwellings in densely populated regions. As shown in Fig. 1, high-rise apartments in Korea consist of thin reinforced concrete (RC) walls that support slabs without beams and columns. This feature may be attributed to the aim of maximizing the service area and construction efficiency to shorten the work period.

The RC bearing walls in this type of buildings can be characterized by the following: a deep rectangular section with a high aspect ratio (height-depth ratio); a considerably smaller amount of steel than the usual column sections; an unexpectedly low level of confinement of the concrete; and a high axial loading.

The structural validity of a building with this type of bearing wall and slab system has been empirically verified against gravity and wind loading. However, little is known about its ultimate behavior under an earthquake loading because severe ground motion has not been experienced in Korea in recent generations. Furthermore, few experimental studies have been reported on this structural system because of the excessively large prototype that must be accommodated in a laboratory for testing the destruction. It is crucial therefore to analytically predict such behavior on the basis of appropriate assumptions and rational mechanisms. Although a few analytical models to

† Associate Professor, E-mail: kimjh@ajou.ac.kr

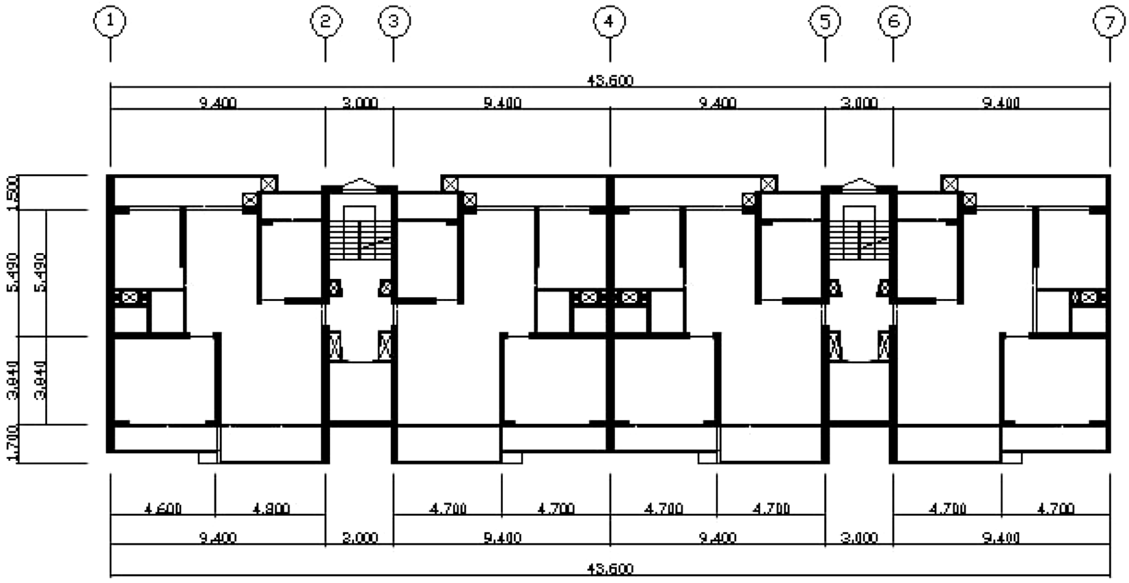

Fig. 1 Plan of typical RC bearing wall-slab apartment

investigate the behaviour of RC walls were reported for cyclic quasi-static loading(Kwak and Kim 2004) and for dynamic loading(Fischinger, *et al.* 2004), these works suggested little design significance. When a bearing wall of a high-rise apartment building is deformed by an earthquake, some large flexural-compressive strains are likely to develop at the end of the wall over the critical section due to the wall's high aspect ratio, its thickness, and the existence of an axial loading. Such a large deformation demand may cause the concrete to be prematurely crushed at the compression end; and, thus, the ductility of the structural system may be limited. To secure and enhance the ductility capacity of the bearing wall system in the face of severe deformation, the deformability of concrete in compression should be enormously improved, or the neutral axis depth in flexures should be reduced for a given ultimate strain in the compressive extreme fiber.

In seismic design, one of two options may be used: first, the concrete must be confined in the compression end zone as practiced in columns (Mander, *et al.* 1988); alternatively, boundary elements must be provided at both ends to ensure the wall has a barbell-shaped cross section (ACI 2002). These options should improve the flexural deformability. In addition, if necessary, the unwanted shear failure can be suppressed by adding diagonal web reinforcement (Sittipunt and Wood 2000).

The confinement option can be considered a space problem because the RC wall section may not be spacious enough to accommodate the confining steel or to activate the confinement effect due to its limited thickness. In this situation, however, the boundary element option is advocated as long as the architectural requirement is not violated.

The current state-of-the-practice (ACI 2002) requires the provision of boundary elements to a wall system that is subjected to the intensive ground motion of strong earthquakes. However, the current practice does not suggest how to rationally and efficiently dimension the section of boundary elements.

The significance of applying these options to thin walls is now discussed and a comprehensive way dimensioning the boundary elements is proposed in what follows.

2. Current design practice

In accordance with the current design practice (ACI 2002, KCI-AIK 1999) for low to moderate seismic regions, RC bearing walls are designed as cantilever columns that can be subjected to axial loading and moment. The required minimum thickness is 100 mm and the required minimum steel quantity is 0.0012 and 0.002 of the gross section for vertical and horizontal directions, respectively. The maximum space between bars in both vertical and horizontal directions is the lesser of 400 mm and three times the wall thickness. For walls in high seismic regions, the ACI (2002) requires boundary elements with adequate transverse steel for confinement of the concrete.

In Korean practice, the RC bearing walls in a wall-slab building system are typically 3 m to 10 m deep and 150 mm to 200 mm thick. The typical story height is 2.6 m, resulting in a H/L aspect ratio of 3 to 28 in a 12-story apartment building. The average dead loads are 5.3 kN/m^2 and the live loads are 2 kN/m^2. From this scenario, as shown in Fig. 2, the range of axial load ratios at the critical section for $1.0D$+$0.25L$ is $P/f_c' A_g = 0.05 \sim 0.4$ in most cases. The typical reinforcement is D10@200 mm~300 mm placed in double layers, and this reinforcement gives steel ratios of 0.0018 to 0.0025 for both the vertical and horizontal directions. The wall end zones are typically reinforced with vertical bars of 4-D13, 6-D16 or 6-D19. In addition, U-bars with the same spacing as the horizontal bars are placed as shown in Fig. 3. Such details for wall ends have been traditionally and empirically used without any theoretical verification.

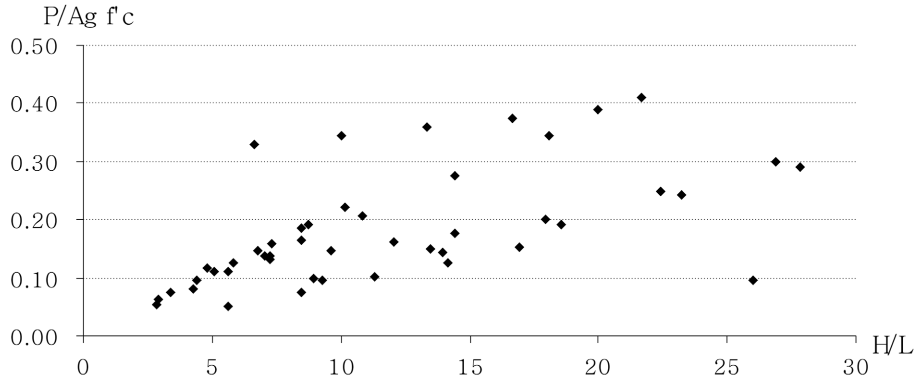

Fig. 2 Axial load ratios over various aspect ratios (1.0D+0.25L)

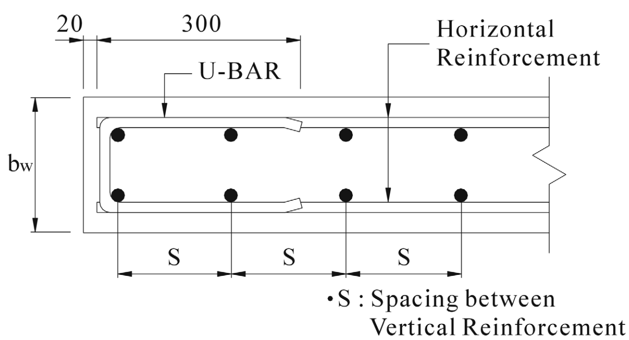

Fig. 3 Typical detail of bearing wall ends in Korean Practice

3. Adequacy of confining the compression end

The confinement of concrete in a column subjected to high axial loading can effectively enhance the behavior of the concrete by extending the ultimate stage. The confinement effect, which is exerted by reinforcing steel that surrounds the core concrete, is activated when the reinforcing steel is subjected to tension caused by the lateral expansion of the core concrete.

The benefit of confinement in columns has been verified. However, whether the same benefit can be expected in thin walls is not known yet and should be investigated. Of the various models used to evaluate the confinement effect, a comprehensive model was selected for this purpose. Mander, *et al*. (1988) proposed a theoretical expression to determine the confinement effect due to transverse reinforcement for rectangular and circular columns. In its general form, the confinement effect on the stress-strain curve of concrete can be expressed by

$$K = f'_{cc}/f'_{co} \tag{1}$$

$$\varepsilon_{cc} = \varepsilon_{co}[1 + 5(K - 1)] \tag{2}$$

where K is the factor of confinement effect, f'_{cc} and ε_{cc} are the stress and strain at the peak of the confined concrete, and f'_{co} and ε_{co} are the stress and strain at the peak of the unconfined concrete. With the improved stress-strain curve of concrete due to confinement, the rotational capacity at the critical section of the wall can be enhanced; that is, $\phi_u = \varepsilon_{cu}/c$, where ε_{cu} is the strain at the ultimate stage. Thus the ductility can also be enhanced. In applying this model to the compression end of the bearing walls, a slight modification is required, as shown in Fig. 4, because no cover concrete will be spalled out from the compressed concrete that contacts with the neutral axis.

The design variables used to determine K are the yield strength of the steel, the dimensions of the confined section, the bar diameter, and the spacing of the vertical and horizontal steel. The mathematical expressions used to obtain K from the design variables are intentionally omitted to avoid repetition because they are available elsewhere (Mander, *et al.* 1988). Fig. 5 presents the factor of confinement effect, along with the net space between the vertical bars, for various arrangements of the transverse steel and wall thickness. For a parametric study, b_c = 600 mm for the confined portion of the wall and the following values are assumed: f'_c = 30 MPa and f_y = 400 MPa. The wall thicknesses of 150 mm, 200 mm and 250 mm are considered. The arrangement of the transverse reinforcement with D10@50, @100, @150 and @200 is also considered. The factor of confinement effect K can then be directly read from the Fig. 5 when the

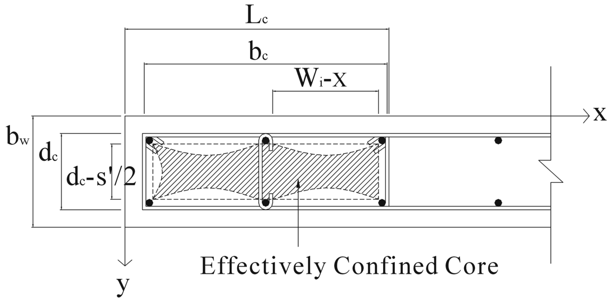

Fig. 4 Confinement of compression end of a wall

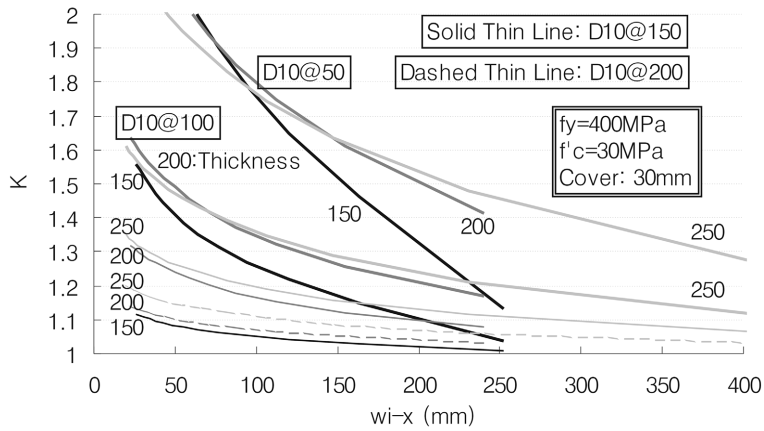

Fig. 5 Factor of confinement effect influenced by various factors

wall thickness and the arrangements of the transverse and longitudinal steel are given.

The parameter that has the greatest influence on the confinement effect is the spacing between the transverse steel, though the variation diminishes as the space between the longitudinal steel increases. The threshold of the spacing between the bars and the wall thickness for a confinement measure depends on the relativity between the design variables for K. For example, to obtain the value of the confinement effect, say $K \geq 1.1$, the threshold of the spacing between the steel bars is D10@200 in the transverse direction with D10@100 in the longitudinal direction, or D10@150 in the transverse direction with D10@200 in the longitudinal direction. In either option, the wall thickness should not be less than 200 mm. Because the space between the longitudinal steel bars is one of the influential parameters, the provision of tie bars is a must. This requirement indicates that in the current Korean practice of thin RC bearing walls the confinement effect cannot be expected to produce a significant level of ductility.

4. Determination of the compression zone

For maximum efficiency, materials should be used in accordance with their natural characteristics. Therefore, it is necessary to appropriately determine the range of the compression zone over the wall section. For this, consider a wall section subjected to axial loading and moment at the ultimate stage, as shown in Fig. 6. The linear strain distribution along the section depth is imposed, and it is assumed that the vertical reinforcement, uniformly distributed over the section, yields either in tension or in compression. The neutral axis depth that is normalized by the overall depth of the wall, c/L, can then be defined by the force equilibrium ($\Sigma F = 0$)over the section. That is

$$\frac{c}{L} = \frac{P/f_c' A_g + \rho_t f_y/f_c'}{\alpha\beta + 2\rho_t f_y/f_c'} \tag{3}$$

where $P/f_c' A_g$ is the axial load ratio, f_c' is the compressive strength of the concrete, f_y is the yield strength of the steel, A_g is the gross section area of the RC bearing wall and ρ_t is the ratio of the longitudinal steel section area to the gross section area of the concrete wall.

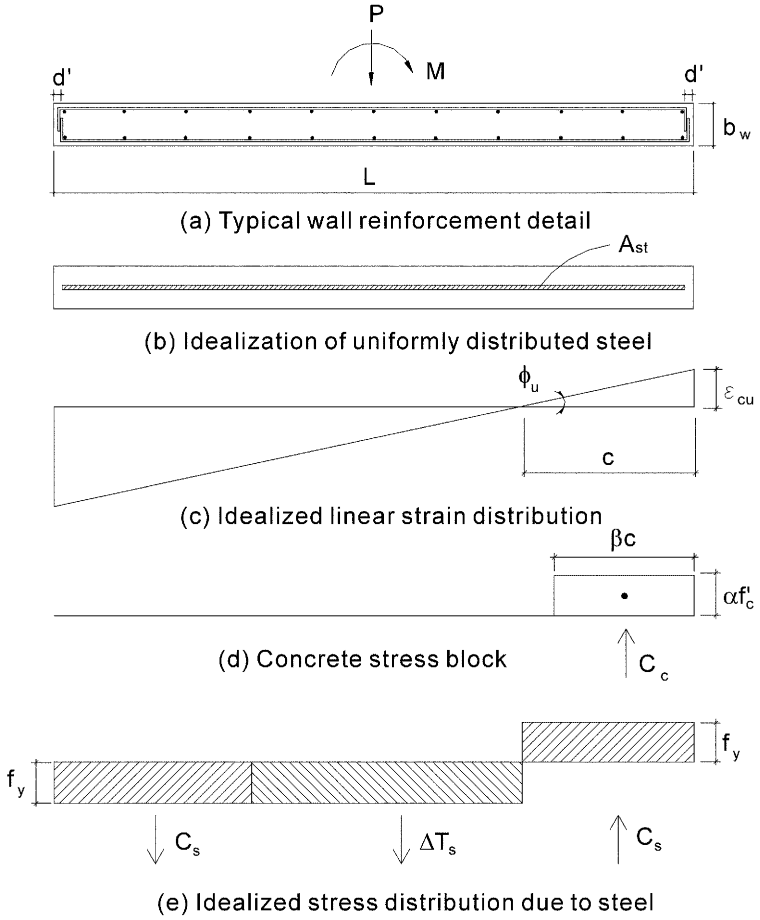

Fig. 6 RC bearing wall section under in-plane flexure at ultimate state

The expression of the neutral axis depth ratio given in Eq. (3) is similar to that in ACI 318-71 (Cardenas, *et al.* 1973) with the exception of the concrete stress block parameters α and β. The ACI suggests that the rectangular stress block parameters be selected as $\alpha = 0.85$ and $\beta = 1.09 - 0.008f_c'$ (in MPa) and $0.65 \le \beta \le 0.85$ when the extreme compressive fiber strain at the ultimate stage is $\varepsilon_{cu} = 0.003$. However, by the first principle, α and β should be determined by the stress-strain model of the concrete, the peak compressive strength f_c' and the extreme compression fiber strain at the ultimate stage. The extreme compression fiber strain, in particular, should be determined by the displacement demand imposed on a RC bearing wall system for site-specific earthquakes.

In seismic design and analysis, it should be assumed that structures and structural elements are likely to be subjected to large deformations. Given this assumption, the larger ultimate compressive strains, ε_{cu}, at the extreme fiber in the compression beyond the prescribed value of 0.003 are considered by different researchers. For the maximum fiber strains in the compression, Paulay and Priestley (1992), as well as Wallace (1995), suggested 0.004, whereas FEMA 273 (1997) suggested 0.005. This implies that the corresponding parameters for the idealization of the rectangular stress block should be modified as well.

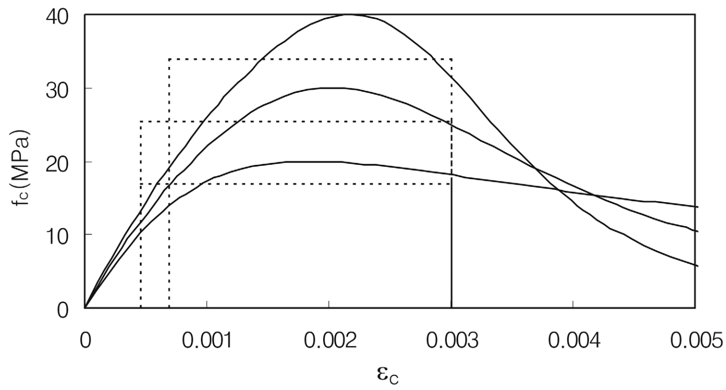

Fig. 7 Stress-strain curves of concrete in compression

4.1. Stress block parameters

The significance of a rectangular stress block is twofold: (1) the area of a rectangular stress block should be the same as the area under the concrete stress-strain curve at the considered maximum strains in compression; and (2) the first moment of the area of a rectangular stress block taken about the neutral axis should be the same as that of the concrete stress-strain curves.

To appropriately evaluate the values of α and β consideration is given to the stress-strain curves of concrete in compression with a maximum strength of 20 MPa, 30 MPa and 40 MPa. In Fig. 7, which shows the stress-strain curves of concrete, the dashed rectangles represent the ACI-idealized stress blocks. For the stress-strain curves of concrete in compression, use is made of Tsai's model as modified by Chang and Mander (1994). For the selected maximum strain at the ultimate stage, the stress block parameters α and β can be determined by

$$\alpha\beta = \frac{\int_0^{\varepsilon_{cu}} f_c \, d\varepsilon_c}{f_c' \varepsilon_c} \tag{4}$$

$$\beta = 2\left(1 - \frac{\int_0^{\varepsilon_{cu}} f_c \, \varepsilon_c d\varepsilon_c}{\varepsilon_c \int_0^{\varepsilon_{uc}} f_c \, d\varepsilon_c}\right) \tag{5}$$

where $\beta \leq 1.0$. Mander, *et al.* (1998) also investigated the rectangular stress block parameters in a similar manner but their work concerned the probable overstrength of bridge columns in flexures.

Fig. 8 plots the parameters $\alpha\beta$ and β in terms of strains normalized by the strain at the peak, ε_{co}, for comparison between different concrete compressive strengths. Table 1 summarizes the values of ε_{co} and $\varepsilon_{cu}/\varepsilon_{co}$ for different concrete strengths. In Fig. 8, the values suggested by the ACI, which were taken at $\varepsilon_{cu} = 0.003$, are marked with solid symbols for comparison. The variation of $\alpha\beta$ and $\varepsilon_c/\varepsilon_{co}$, which follows the stress-strain curves of concrete, indicates that the concrete with the higher strength varies more rapidly than the lower one. While all the values of $\alpha\beta$ are underestimated by the ACI, the $\alpha\beta$ value for $f_c' = 30$ MPa shows the smallest deviation between the ACI results and the results of Eq. (4). The variation of β does not produce a significant

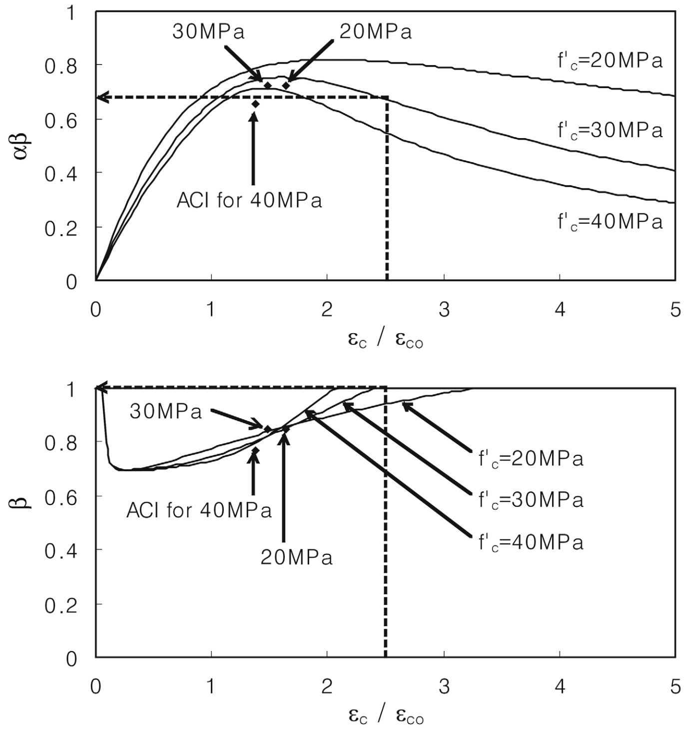

Fig. 8 Stress block parameters for various concrete strengths

Table 1 Strains at the peak and normalized strains under consideration

f'_c(MPa)		20	30	40
ε_{co}		0.001834	0.00203	0.002181
	ε_{cu} = 0.003	1.6357	1.478	1.3754
ε_{cu} / ε_{co}	ε_{cu}= 0.004	2.1809	1.9706	1.8339
	ε_{cu} = 0.005	2.7261	2.4633	2.2924

difference between the curves of different concrete strengths up to $\varepsilon_c / \varepsilon_{co} \approx 1.6$, at which point all the curves meet together. The difference between the curves then becomes larger. Furthermore, although the ACI values for $\alpha\beta$ and β are close to the exact values at the ACI-prescribed $\varepsilon_c / \varepsilon_{co}$, neither the variation in the $\varepsilon_c / \varepsilon_{co}$ values nor the effect of the strain beyond 0.003 could be properly considered. Such a deviation may cause a subsequent probable error when calculating the neutral axis depth ratio *c/L*.

4.2. Compression zone

By incorporating Eq. (4) in Eq. (3), the compression zone, that is, the neutral axis depth ratio c / L, can be plotted in terms of the extreme compression fiber strain for various design variables. In this procedure, the results of which are shown in Fig. 9, the axial load ratio, $P/f_c' A_g$, is 0.0, 0.1 and 0.2; the concrete strength, f_c', is 20 MPa, 30 MPa, and 40 MPa; the yield strength of the reinforcing steel, f_y, is 414 MPa; and the longitudinal steel quantity, ρ_t, is 0.0025 and 0.004. The values calculated with the ACI-prescribed $\alpha\beta$ (Cardenas, *et al*. 1973) are marked with solid symbols.

Also plotted is the c/L suggested by ACI 318-02 (2002) from the study of Wallace (1994) for walls subjected to a large ductility demand. In this case, c/L is determined by the expected maximum lateral drift angle. For the constant axial load ratio ($P/f_c' A_g = 0.1$ in Fig. 9), all the curves plotted by Eq. (3) are close to each other over the range of strains up to $\varepsilon_c/\varepsilon_{co} = 2$. Above this strain, there is an increase in the difference between the curves for different concrete strengths.

The influence of the steel ratio ρ_t on the difference between curves seems almost insignificant for a higher axial load ratio over the entire range of $\varepsilon_c/\varepsilon_{co}$. As implied in Fig. 9, $P/f_c' A_g$ is a more decisive variable for determining c/L than other variables such as f_c', ρ_t and f_y/f_c'. For $P/f_c' A_g = 0.1$, the values of c/L calculated by ACI 318-71 seem close to the exact value at the ACI-prescribed $\varepsilon_c/\varepsilon_{co}$. However, there is a significant deviation in all other $P/f_c' A_g$ values. The values of c/L as determined by ACI 318-02 (2002) for $\delta_h/h_w = 0.01$ approximately coincide with those for $P/f_c' A_g = 0.1$ up to $\varepsilon_c/\varepsilon_{co} = 2$, where δ_h/h_w denotes the maximum lateral drift angle. Above this value, the gap between them gets greater. The values c/L for $\delta_h/h_w = 0.02$ and 0.03 are scattered around those for $P/f_c' A_g = 0.0$ over the entire range. Such a limited coincidence indicates that ACI 318-02 cannot appropriately reflect the effect of all the variables that influence c/L.

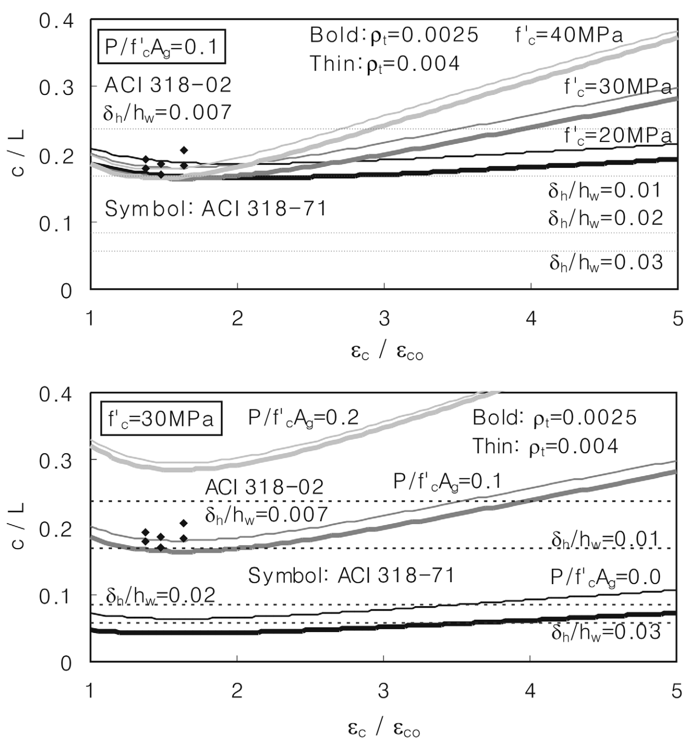

Fig. 9 Compression zone of RC wall subjected to in-plane flexure at ultimate state

5. Dimensioning boundary elements

In a typical wall-slab building system in Korea, the thickness of walls range from 150 mm to 200 mm, and this range may not be spacious enough to accommodate the confinement steel or to activate the confinement effect. An alternative way of enhancing the ductility capacity of RC walls may therefore be required. That is, instead of improving the deformability of concrete by confinement, the neutral axis depth c can be reduced by placing the boundary elements as shown in Fig. 10. Everything else other than the boundary elements is the same as in Fig. 6.

The longitudinal steel in the boundary elements is not expected to reduce c because the internal flexural compressive and tensile forces that are generated at opposite ends cancel each other out. To maximize the efficiency of the boundary element in flexural compression, the entire section of the boundary element should be located within the neutral axis depth, c/L; that is, within the compression zone. By introducing the dimensional factors m and k for the boundary elements, the neutral axis depth that is normalized by the wall depth can be defined, from the equilibrium of forces by

$$\left(\frac{c}{L}\right)_{BE} = \frac{P/f_c' A_g + \rho_t f_y / f_c'}{\alpha\beta(1+mk) + 2\rho_t f_y / f_c'} \tag{6}$$

where m is the ratio of the boundary element depth to depth of the rectangular stress block and k is the ratio of the additional thickness of the boundary element to the wall thickness. To guarantee that the boundary element is located within the compression zone, $m < 1.0$ is required.

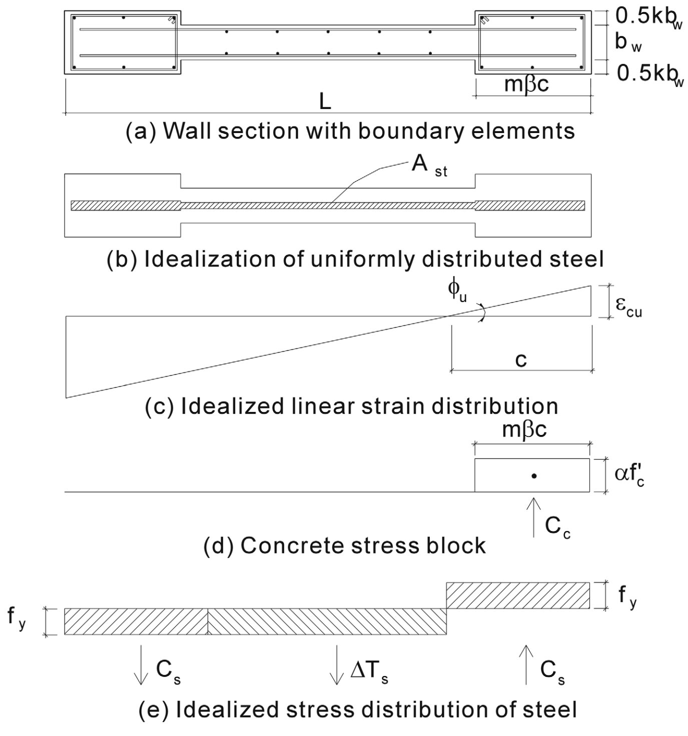

Fig. 10 Section analysis of RC wall with boundary elements

5.1. Design procedure

Fig. 11 presents the plotted compression zone with boundary elements determined by Eq. (6) for various values of *mk*, where $mk = 0$ denotes the wall section without boundary elements. For this presentation, use was made of variables α and β, along with the magnitude of the ultimate strain at the extreme compressive fiber. The compression zone can therefore be extensively decreased by adding the boundary elements, resulting in a ductility enhancement.

Graphs for various values of f_c', ρ_t and $P/f_c' A_g$ can be generated as design charts. With an appropriate value of *mk*, $(c/L)_{BE}$ is readily determined from the chart in Fig. 11. Then, as a final step, *mk* should be decoupled into *m* and *k* in consideration of the architectural aspect, which determines the section dimension of a boundary element. The step-by-step design procedure for the boundary element can be summarized as follows:

Step 1: Select $\varepsilon_{cu}/\varepsilon_{co}$ in consideration of the deformation demand.
Step 2: Determine $\alpha\beta$ and β from the chart in Fig. 8 or Eqs. (4) and (5).
Step 3: Select an appropriate value of *mk*.
Step 4: Determine $(c/L)_{BE}$ from the chart in Fig. 11 or Eq. (6).
Step 5: Decouple *mk* into *m* and *k* in consideration of architectural aspect.
Step 6: The width of the boundary element is $(1+k)b_w$ and the depth is $m\beta c$.

The boundary elements may be treated as extensions of the wall, and Eq. (6) has been derived without considering the confinement effect. If a large deformability in compression is required in the boundary elements, the confining reinforcement can be added for the required confinement effectiveness in accordance with the state-of-the-practice procedure (Mander, *et al.* 1988).

5.2. Worked example

To determine the size of a boundary element, consider an RC bearing wall in which $L = 6000$ mm and $b_w = 200$ mm. Assume that $f_y = 400$ MPa and $f_c' = 30$ MPa ($f_y/f_c' = 13.3$). With $P/f_c'A_g = 0.2$ and $\rho_t = 0.0025$ (0.25 percent), select $\varepsilon_{cu}/\varepsilon_{co} = 2.5$ and $mk = 0.75$. Step 2 produces values of $\alpha\beta = 0.67$ and $\beta = 1.0$ as marked with arrows in Fig. 8. The value of $(c/L)_{BE} = 0.19$ can then be obtained from Step 4, as shown by the arrow in Fig. 11. This value indicates that the neutral axis depth is about 40 percent

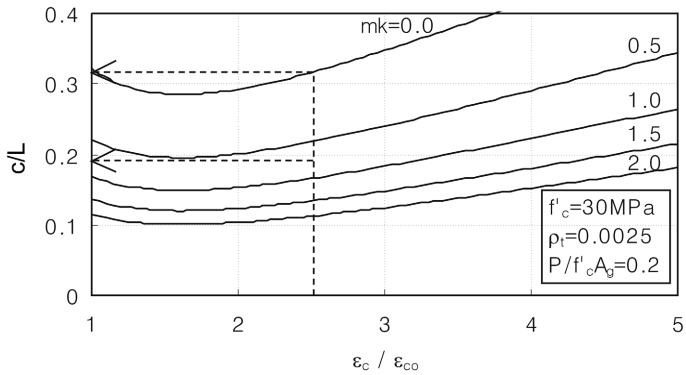

Fig. 11 Compression zone of RC wall with boundary element

less than the value of $c/L = 0.32$ without a boundary element ($mk = 0$). In addition, when $m = 0.75$, k becomes 1.0. The width of a boundary element is calculated by $(1+k)b_w = 2.0 \times 200 = 400$ and, as a final step, the depth is calculated by $m\beta c = 0.75 \times 1.0 \times (0.19 \times 6000) = 855$. The required dimensions of the boundary element are 400 mm × 855 mm.

6. Conclusions

The RC bearing walls of a wall-slab high-rise apartment building subjected to an in-plane flexure were considered for ductility enhancement, and the following conclusions have been drawn:

(1) For confinement to effectively enhance ductility, the spaces between the transverse and longitudinal reinforcing bars and the thickness of the wall should be simultaneously considered. In this case, the provision of tie bars is a must. With the current detailing practice for RC walls in Korea, a significant confinement effect cannot be expected.

(2) A mathematical expression for determining the compression zone of an RC wall at the ultimate stage is proposed in consideration of the concrete stress block parameters governed by the concurrent maximum strain at the extreme compression fiber. The present study indicates that $P/f'_c A_g$ is a more decisive variable for determining c/L than other variables such as f'_c, ρ_l and f_y/f'_c. In particular, with a higher concrete strength and axial load ratio, the variation in the compression zone increases when the strains of the extreme compression fiber are beyond $\varepsilon_{cu}/\varepsilon_{co} = 2.0$.

(3) A comprehensive methodology for dimensioning boundary elements is proposed as an alternative way of enhancing ductility. In this methodology, the size of boundary elements can be determined in consideration of the architectural requirement.

Acknowledgements

The author gratefully acknowledges the partial financial support of the 1999 Fundamental Research Fund of the Korea Science Foundation.

References

ACI 318 (2002), *Building Code Requirements for Structural Concrete and Commentary, American Concrete Institute*, Michigan, U.S.A.

Cardenas, A. E., Hanson, J. M., Corley, W. G. and Hognestad, E. (1973), "Design provisions for shear walls', *ACI J.*, 70-23, March, 221-230.

Chang, G. A. and Mander, J. B. (1994), "Seismic energy based fatigue damage analysis of bridge columns, Part I: Evaluation of seismic capacity", Technical Report NCEER-94-0006, National Center for Earthquake Engineering Research, State University of New York at Buffalo, New York, U.S.A.

FEMA 273 (1997), *NEHRP Guidelines for the Seismic Rehabilitation of Buildings*, Building Seismic Safety Council.

Fischinger, M., Isakovic, T. and Kante, P. (2004), "Implementation of a macro model to predict seismic response of RC structural walls", *Comput. and Concrete, An. Int. J.*, **1**(2), 211-226.

KCI-AIK (1999), *Reinforced Concrete Structural Design Standards*, Korea Concrete Institute and Architectural Institute of Korea, in Korean.

Kwak, H. G. and Kim, D. Y. (2004), "Cracking behavior of RC shear walls subjected to cyclic loading", *Comput. and Concrete, An. Int. J.*, **1**(1), 77-98.

Mander, J. B., Priestley, M. J. N. and Park, R. (1988), "Theoretical stress-strain model for confined concrete", *J. Struct. Eng., ASCE,* **114**(8), August, 1804-1825.

Mander, J. B., Dutta, A. and Goel, P. (1998), "Capacity design of bridge piers and the analysis of overstrength", Technical Report MCEER-98-0003, Multidisciplinary Center for Earthquake Engineering Research, State University of New York at Buffalo, New York, U.S.A.

Paulay, T. and Priestley, M. J. N. (1992), *Seismic Design of Reinforced Concrete and Masonry Buildings*, Wiley.

Sittipunt, C. and Wood, S.L. (2000), "Development of reinforcement details to improve the cyclic response of slender structural walls", *Proceedings of 12th World Conference of Earthquake Engineering*, Paper id. 1770, Auckland, New Zealand.

Wallace, J. W. (1994), "New methodology for seismic design of RC shear walls", *J. Struct. Eng.*, *ASCE*, **120**(3), March, 863-884.

Wallace, J. W. (1995), "Seismic design of RC structural walls, Part I: New Code Format", *J. Struct. Eng.*, *ASCE,* **121**(1).

CC